AUT Journal of Civil Engineering

AUT J. Civil Eng., 8(2) (2024) 109-126
DOI: 10.22060/ajce.2025.23539.5881

# Comparative Analysis of Multi-Linear Lag Cascade Model with Advanced Hydrological Techniques for Flood Prediction in Zarineh Rud River, Iran

Jafar Chabokpour *

Department of Civil Engineering, University of Maragheh, Maragheh, Iran.

**ABSTRACT:** The study focuses on the detailed methods of flood prediction in the Zarineh Rud River within Urmia Lake, Iran. It compared five different methods: the Multi-Linear Lag Cascade model, Saint-Venant equations, and three soft computing methods, namely Artificial Neural Networks, Adaptive Neuro-Fuzzy Inference System, and Support Vector Machines. In this study, the data of the 2022 flood recorded at Alasaql and Safakhaneh stations were used. The performances of the models were then evaluated in terms of various statistical criteria such as the Nash-Sutcliffe Efficiency (NSE), Root Mean Square Error (RMSE), Peak Flow Ratio (PFR), and Percent Error in Peak (PEP). In general, it was found that the soft computing techniques, in particular ANN and ANFIS, are representing the best performance with NSE values of 0.938 and 0.935, respectively. Similarly, the MLLC model showed competitive performance with a value of NSE equal to 0.922 but with much lower computational time. The Saint-Venant model was somewhat less accurate, with an NSE value of 0.901 but with higher robustness against input uncertainty. For all models, results are better for the high flow range which is of importance for flood forecasting. Sensitivity analysis has shown that soft computing methods are more sensitive to input data errors than physically based Saint-Venant. This work underlines several critical trade-offs when optimizing model accuracy, computational efficiency, and robustness to uncertainty for flood prediction. The results highlight that soft computing methods, particularly ANN and ANFIS, are recommended for applications requiring high prediction accuracy and where high-quality input data is available. These insights can directly inform the development and implementation of flood warning systems in the Zarineh Rud River basin and similar hydrological systems worldwide.

**Review History:**

Received: Sep. 19, 2024
Revised: Dec. 19, 2024
Accepted: Jan. 15, 2025
Available Online: Jan. 15, 2025

**Keywords:**

Multi-Linear Lag Cascade Model
Flood Prediction
Soft Computing Methods
Saint-Venant Equations
Zarineh Rud River

## 1- Introduction

Flood routing in river reaches is indeed an important part of hydrological modeling and has become very helpful in flood wave prediction and flood risk management. It is actually all about finding out the time of water flow and the magnitude as it moves downstream in river channels. The processes involved are influenced by various factors, including channel geometry, flow resistance, and upstream inflow conditions. The Muskingum method, by reason of its simplicity and capability to handle sizable hydrological processes, remains one of the most utilized techniques for flood routing. This technique, in conjunction with some other methods, stands very important to understanding and predicting the flood behavior that plays a vital role in floodplain management and planning infrastructure [1-4]. Generally, flood routing methods may be classified as hydrologic and hydraulic approaches. Hydrologic methods, of which the Muskingum model is one such application, use the continuity equation and are favored in practice by virtue of ease and lower data demands [1, 5-7]. They find greater use in ungauged basins where data is limited [8]. On the other hand, hydraulic methods, including the St. Venant equations, are capable of finer detail and incorporate the physical features of the river channel in the simulation; however, they do require a great deal of data to operate [9-12]. Very recently, some new developments included the use of genetic programming in conjunction with traditional methods for improving the accuracy of flow forecasts in complex river systems [13]. Global hydrological models have also been extended to include advanced routing schemes like that of CaMa-Flood, which includes floodplain storage and backwater effects, thus providing an improved simulation of peak river discharges [14]. Besides the technical challenge, flood routing is an important methodological and strategic problem when managing floods. The accuracy of flood prediction and the effectiveness of proposed flood mitigation can differ significantly with the chosen routing method [15]. The conceptual approach of the cell in-series model of flood routing involves dividing any reach of the river into a lot of interconnected cells, with each cell representing a segment of the river. It is an effective model

*Corresponding author's email: J.chabokpour@maragheh.ac.ir

used to simulate flood waves throughout river systems as a result of the cumulative impacts that each cell exerts on the general system's flow dynamics. In view of this, the model is useful for simulating flood wave advancement through river systems, as it considers the cumulative impacts of each cell on the overall flow dynamics [16, 17]. The cells in the series model enhance the accuracy of flood routing by segmenting a river reach into more intervals or cells for an enriching representation of flow dynamics. Such segmentation enables the model to capture the spatial variability of the river's characteristics, which is quite fundamental in developing a proper representation of flood-wave movement [18, 19]. The MLLC (The Multi Linear Lag Cascade) model is one of the complicated methods of flood routing in river reaches, which has been proposed for a more precise estimation of flood waves. It will be very useful in light of the simulation of the complex dynamics of flood propagation, considering more series reservoirs with different lags. The capability for temporal distribution of flow that MLLC represents makes the model beneficial in flood management and planning [20]. Application is paramount, especially where reliable flood forecasting forms a basis for devising appropriate mitigation strategies for flooding impacts on both communities and infrastructural investments, among other resources sensitive to flooding [21]. The MLLC model improves the basis of the traditional flood routing method because it includes more detail about the flow process with multiple linear reservoirs. This method enhances the accuracy in forecasting a flood more than simpler models, such as the Muskingum method. The flexibility in the number of reservoirs and relative lag times permits its tailoring for specific river characteristics, extending further its applicability to a wide range of hydrological setups [22, 23]. In recent works, optimization algorithms such as the Whale Optimization Algorithm have been incorporated to determine the optimal parameters of the MLLC model and further improve its performance in solving flood routing problems. These newer methods have indeed reported more substantial enhancements in the accuracy of flood wave simulations, particularly for ungauged catchments where data is scarce [23, 24]. The MLLC model proves quite robust regarding the handling of lateral inflow and boundary variation in river conditions throughout a flood event. It has also been applied to real-time flood predictions, yielding quite satisfactory results in several case studies undertaken so far, hence demonstrating its ability to provide good forecasts that could be supportive of proper flood management strategies [25, 26]. The MLLC model represents another leap in the methods of flood routing techniques, hence providing an increase in accuracy and flexibility within the routing of river floods. In some instances, it has already been applied to ungauged catchments, and it will therefore be able to provide flood predictions that are quite accurate in data-scarce environments as well [21]. The methods of soft computing have become very popular for flood routing in the reaches of rivers due to their capability to deal with complex and nonlinear systems with scarce data. Some of the used techniques are artificial neural networks, genetic algorithms, ant colony optimization, and particle swarm optimization -techniques that have already seen effective applications in flood hydrograph prediction. These methods, besides being superior to conventional techniques, reduce error in peak discharge and time to peak, hence powerful tools for flood prediction [27]. It has also been found in the literature that traditional models, such as the Muskingum method, have been combined with optimization algorithms. For instance, some researchers have applied the Improved Bat Algorithm for the three-parameter calibration of the Muskingum model and achieved a drastic improvement in the accuracy of flood routing forecasts. Such an approach possibly underlines the potential benefits that may be derived from embedding soft computing into traditional hydrologic models in order to further develop flood forecasting [20]. Neural networks have been applied to flood routing in rivers, providing a simpler alternative to solve the complex Saint Venant equations. Such models require less data and less computational effort, hence suitable for real-time applications. The application of neural networks in flood forecasting has provided promising results and acceptable ranges of error between observed and simulated flood hydrographs [28]. Besides, soft computing methods for parameter optimization have been suggested to be a very attractive alternative to conventional survey work, which is often costly and time-consuming. Optimization methods are effective in determining geometric and hydraulic properties of river reaches, enhancing accuracy in flood routing models [29].

Due to its simplicity and efficiency, the MLLC model has found wide applications in many hydrological studies. However, the performance of this model compared with advanced methods has not been comprehensively investigated in complex river systems using Saint-Venant equations and soft computing techniques. This paper presents the application of the MLLC model for flood prediction in the Zarineh Rud River, Iran. Therefore, the research objectives are related to the performance evaluation of the methods in terms of their accuracy, computational efficiency, and robustness under the different regimes of flow and uncertainties in input, thus developing guidelines on choosing appropriate flood prediction models under similar hydrological contexts.

Recent studies have demonstrated significant advancements in flood prediction methodologies. Kumar et al. [30] have shown that machine-learning approaches can effectively improve flood forecasting accuracy in complex river systems. The importance of model comparison and validation has been further emphasized by Zang et al. [31] who conducted comprehensive evaluations of different routing schemes. Meresa et al. [32] have made notable contributions in uncertainty analysis for flood prediction models, while Koutsovili et al. [33] have demonstrated innovative approaches to real-time flood forecasting. Additionally, the work of Li et al. [34] has provided new insights into the integration of multiple data sources for improved flood prediction accuracy.

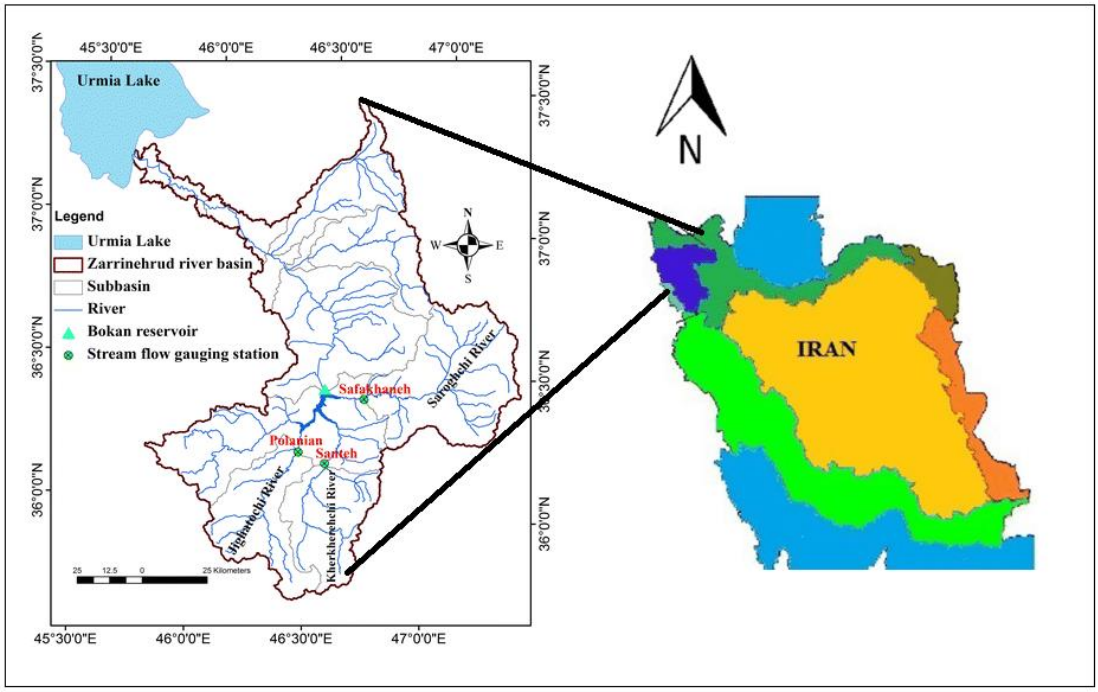


**Fig. 1. Location of the Zarrine river basin in Iran**

## 2- Materials and methods

### 2- 1- Study Area Characteristics and Data Collection

In this study, Data from the Zarineh Rud River in the Urmia Lake basin were used to study a wide range of flood prediction methods in depth. This dataset includes hourly inflow and outflow at Alasaql and Safakhaneh stations, respectively, in 2022 (Fig. 1). The Zarineh Rud River, located in northwestern Iran, is the largest river flowing into Lake Urmia, with a total length of approximately 302 kilometers and a drainage area of 11,578 square kilometers. The river basin lies between 35°45' to 37°20' N latitude and 45°45' to 47°20' E longitude. The climate in the study area is characterized as semi-arid to cold semi-arid, with average annual precipitation ranging from 300 to 400 mm, predominantly occurring between October and May. The hydrometric data used in this study were collected from two primary monitoring stations: Alasaql station (upstream, 36°37'N, 46°23'E) and Safakhaneh station (downstream, 36°51'N, 46°08'E), with a river reach length of approximately 42.5 kilometers between them. Both stations are equipped with water level sensors (accuracy ±1 cm) and automated data logging systems that record water levels. The stage-discharge relationships at both stations are regularly updated through monthly discharge measurements. Quality control procedures were implemented to ensure data reliability, including automated range checks, consistency tests, and manual verification of unusual values. The river reach under study has an average width of 45 meters and a mean slope of 0.002 m/m, with predominantly gravel-bed composition and minimal lateral inflows.

### 2- 2- Methodology and Model Development

Five different methods for flood prediction were investigated; those are MLLC model (Multi-Linear Lag Cascade), Saint-Venant equations, ANN (Artificial Neural Networks), ANFIS (Adaptive Neuro-Fuzzy Inference System), and SVM (Support Vector Machines). In this paper, a conceptual hydrological model known as the MLLC was applied to forecast outflow using a sequence of lagged inflows. The model, provided by Eq. 1, Fig. 2.

$$Q_{out}(t) = \sum_{i=1}^{n} \left(a_i \, Q_{in}\,(t - i\Delta t)\right) + b \qquad (1)$$

Where $Q_{out}(t)$ is the outflow at time t, $Q_{in}(t - i\,\Delta t)$ is the inflow at time t-iΔt, $a_i$ are the model parameters, b is the base flow, and n is the number of lag times considered. The optimal number of lag times was determined through an iterative process, evaluating model performance for increasing n values.

The numerical solution of the Saint-Venant equations governing one-dimensional unsteady flow was performed by using the MacCormack scheme. The Saint-Venant equations can be expressed as continuity Eq. 2 and momentum Eq. 3. The schematic of model operation and equation connections is presented in Fig. 3.

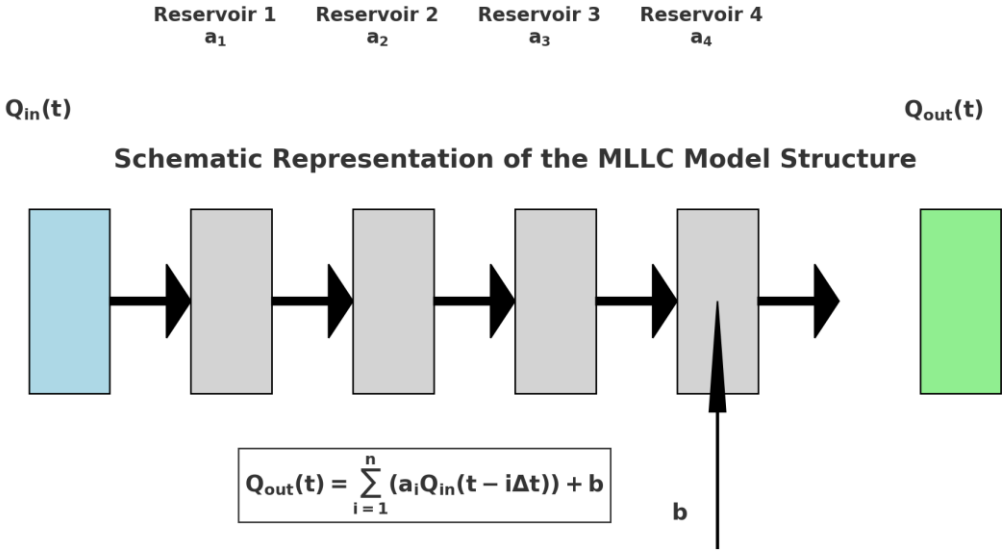


Fig. 2. Schematic representation of the MLLC model structure

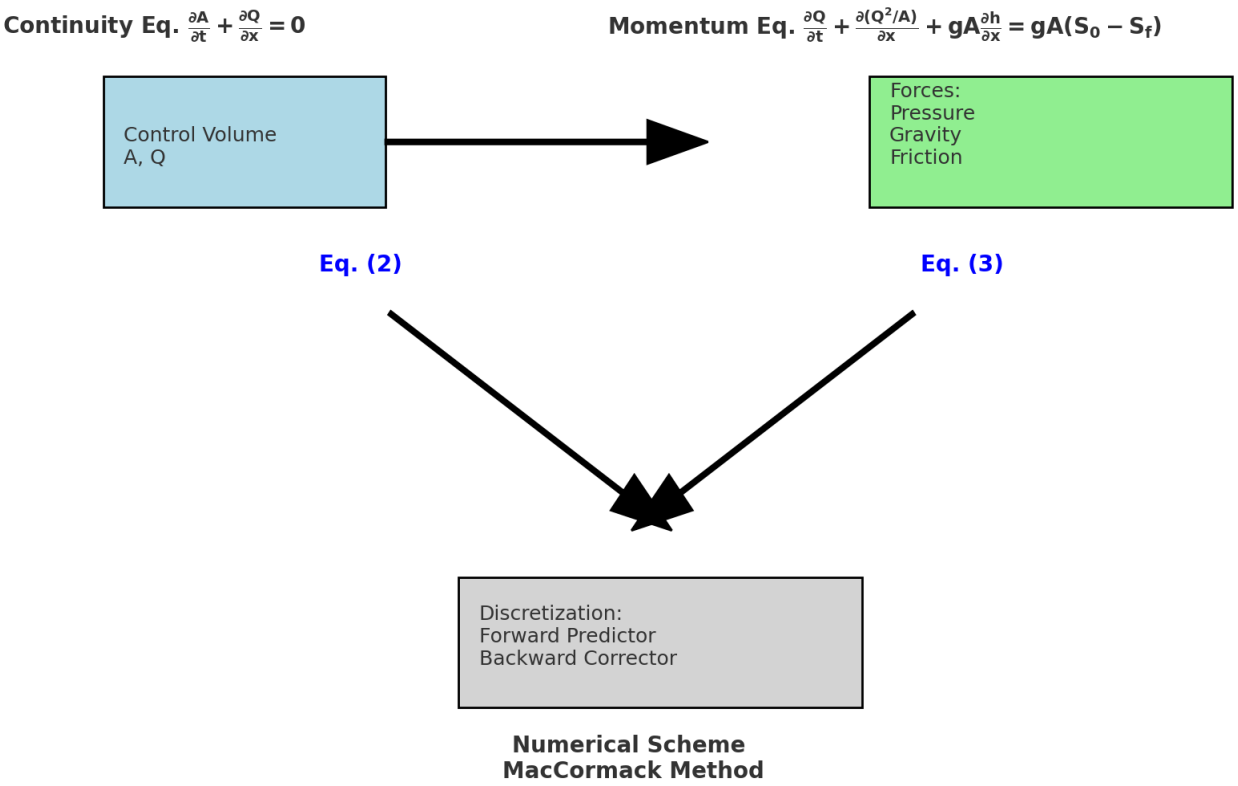


Fig. 3. Schematic representation of the Saint-Venant equations

$$\frac{\partial A}{\partial t}+\frac{\partial Q}{\partial x}=0 \quad (2)$$

$$\frac{\partial Q}{\partial t}+\frac{\partial\left(\frac{Q^2}{A}\right)}{\partial x}+ gA\frac{\partial h}{\partial x}=gA(S_0-S_f) \quad (3)$$

Where A is the cross-sectional area, Q is the discharge, h is the water depth, $S_0$ is the bed slope, $S_f$ Is the friction slope, and g is the gravitational acceleration.

The ANN model was realized in the form of a feedforward neural network with one hidden layer. The number of hidden neurons in this layer was determined by trial and error. The training was carried out using the Levenberg-Marquardt algorithm: the input layer consisted of lagged inflow values, while the output layer stands for the predicted outflow.

The ANFIS model was developed based on neural networks and fuzzy logic using a Sugeno-type fuzzy inference system. Then the number of membership functions was optimized for best performance. The structure of the model can be described as Eq. 4.

$$Q_{out}(t)=\sum_{i=1}^{n}(w_i\, f_i\, Q_{in}) \quad (4)$$

where $Q_{out}(t)$ represents the predicted outflow at time t, $w_i$ denotes the normalized firing strengths of the fuzzy rules (representing the degree of activation of each rule, with values between 0 and 1), $f_i$ represents the consequent functions (linear combinations of input variables determined during the training process), $Q_{in}$ is the input flow, and n is the total number of fuzzy rules in the system. The firing strengths $w_i$ are computed through the fuzzy inference process using membership functions optimized during the training phase.

The SVM model was implemented using a radial basis function (RBF) kernel. The SVM regression function is expressed as Eq. 5.

$$f(x)=\sum_{i=1}^{n}(\alpha_i\times\alpha_{i^*}\times K(x_i,x))+b \quad (5)$$

where f(x) is the predicted output, $\alpha_i$ and $\alpha_{i^*}$ are the Lagrange multipliers obtained through the optimization process (representing the contribution of each training sample to the final model), $K(x_i, x)$ is the Radial Basis Function (RBF) kernel that maps the input space to a higher-dimensional feature space (defined as $\exp(-\gamma||x_i - x||^2)$, where $\gamma$ is the kernel parameter), $x_i$ represents the support vectors selected during training, x is the input vector, b is the bias term determined during model optimization, and n is the number of support vectors. The parameters $\alpha_i$, $\alpha_{i^*}$, and b is optimized during the training process to minimize the prediction error while maintaining model generalization capability. Schematic of operated soft computing methods is presented in Fig. 4.

While this study utilizes established hydrological models, The methodological innovation lies in the comprehensive evaluation framework we developed. This framework uniquely combines performance assessment across flow regimes, computational efficiency analysis, and uncertainty quantification through Monte Carlo simulation. The novelty of our approach is further enhanced by the systematic investigation of model behavior under different input uncertainty scenarios, which provides valuable insights for practical applications in data-scarce regions. Our methodology introduces a new perspective on model selection by considering not only traditional performance metrics but also the practical constraints of real-time flood forecasting applications. This comprehensive evaluation framework can be adapted and applied to other river systems, particularly in semi-arid regions with similar hydrological characteristics.

The performance of all models was evaluated based on the following metrics: Nash-Sutcliffe Efficiency (NSE), RMSE (Root Mean Square Error), Peak Flow Ratio (PFR), Percent Error in peak (PEP); mathematically defined in Eqs. 6-9.

$$NSE=1-\frac{(\sum_i^m(Q_{obs.i}-Q_{sim,i})^2)}{(\sum_i^m(Q_{obs.i}-\bar{Q}_{obs})^2)} \quad (6)$$

$$RMSE=\frac{(\sum_i^m(Q_{obs.i}-Q_{sim,i})^2)}{m} \quad (7)$$

$$PFR=\frac{Q_{p,sim}}{Q_{p,obs}} \quad (8)$$

$$PEP=\frac{(Q_{p,sim}-Q_{p,obs})}{Q_{p,obs}}\times 100 \quad (9)$$

Where $Q_{obs.\,i}$ and $Q_{sim,i}$ are the observed and simulated flows at time i, $\bar{Q}_{obs}$ is the mean observed flow, m is the number of observations, and $Q_{p,\,sim}$ and $Q_{p,\,obs}$ are the simulated and observed peak flows, respectively.

Thus, based on the regime of flow, the dataset was divided into low flow (< 25th percentile), medium flow ($25^{th}$ to $75^{th}$ percentile), and high flow (> $75^{th}$ percentile). The NSE was computed for each of the flow regimes.

Sensitivity analysis was then performed to evaluate the strength of the models with respect to uncertainty in

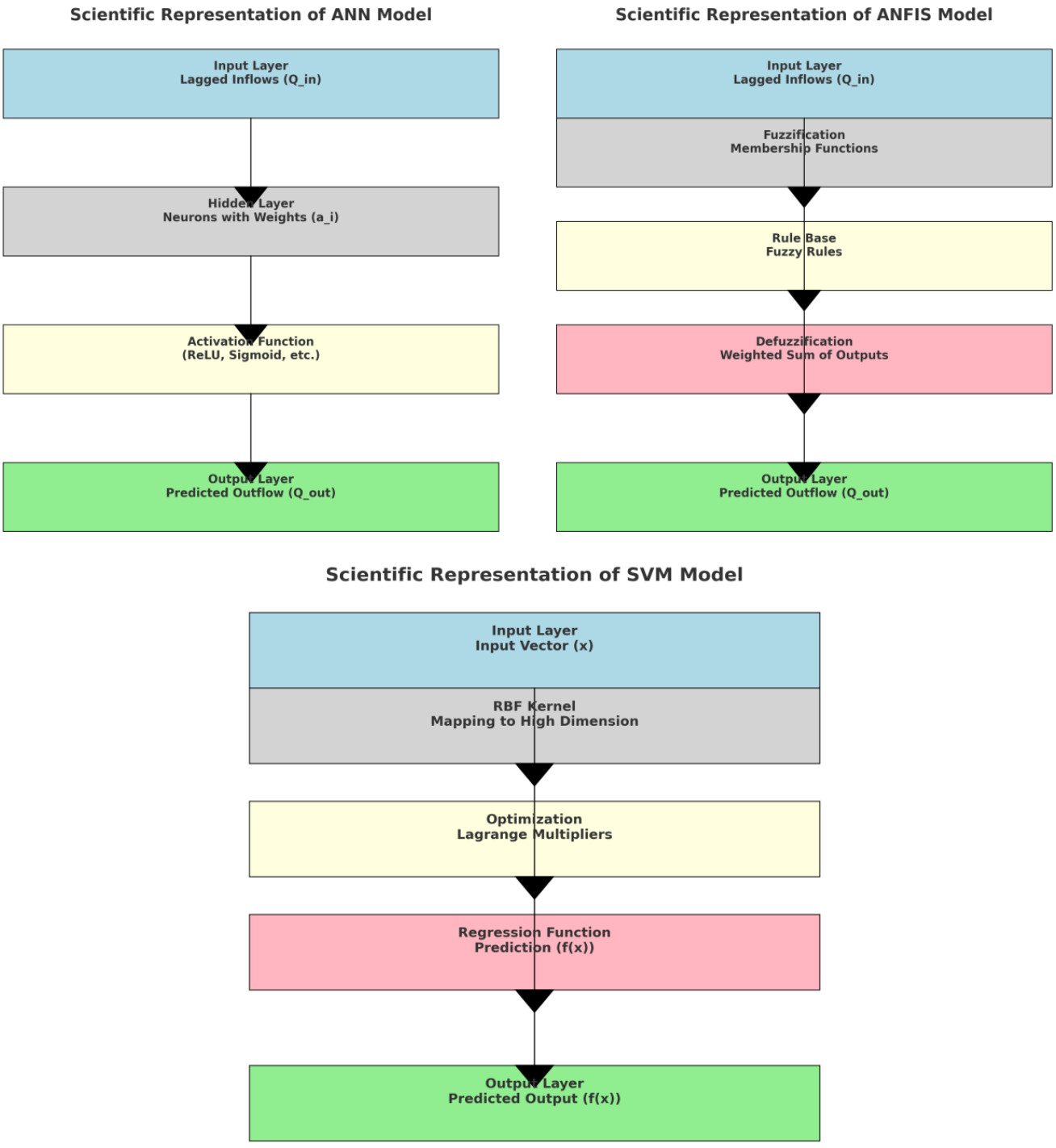


**Fig. 4. Architecture of the implemented soft computing models**

**Table 1. MLLC Model Performance for Different Lag Times**

| n | NSE | RMSE ($m^3/s$) |
|---|---|---|
| **1** | 0.7823 | 8.42 |
| **2** | 0.8456 | 6.73 |
| **3** | 0.8912 | 5.18 |
| **4** | 0.9134 | 4.32 |
| **5** | 0.9287 | 3.86 |
| **6** | 0.9315 | 3.79 |
| **7** | 0.9318 | 3.78 |
| **8** | 0.9319 | 3.78 |
| **9** | 0.9319 | 3.78 |
| **10** | 0.9319 | 3.78 |

the inputs. To that end, Monte Carlo simulations of peak flows were run by adding random errors with an increasing standard deviation (from 1% up to 5%) to the input data. The coefficient of variation (CV) of simulated peak flows was calculated as an uncertainty measure (Eq. 10).

$$CV = (\sigma/\mu) \times 100\% \quad (10)$$

Where σ is the standard deviation of the simulated peak flows, and μ is the mean.

## 3- Results

### 3- 1- Model Performance and Statistical Analysis

In the present study, the flood routing of the Zarineh Rud River was routed by using the MLLC (Multi-Linear Lag Cascade ) model, which is particularly capable of representing the relationship between the upstream and downstream flows in river systems. The number of lag times 'n' could be determined by an iterative process. The model performance for n ranging from 1 to 10 was assessed using the Nash-Sutcliffe Efficiency (NSE), and Root Mean Square Error criteria (RMSE). The results of this analysis are given in Table 1.

These results showed that n=6 was the optimal tradeoff between model complexity and improvement in model performance. No further improvement in model performance was achieved for n > 6. The parameters of the MLLC model, $a_i$ and b were determined by the least squares method. The objective function to be minimized was given by Eq. 11.

$$\min \sum_{t=1}^{t=T} (Q_{out}{}^{obs}(t) - Q_{pred}{}^{obs}(t))^2 \quad (11)$$

**Table 2. Optimized MLLC Model Parameters**

| Parameter | Value |
|---|---|
| $a_1$ | 0.3241 |
| $a_2$ | 0.2876 |
| $a_3$ | 0.1952 |
| $a_4$ | 0.1103 |
| $a_5$ | 0.0584 |
| $a_6$ | 0.0244 |
| **b** | 1.8735 |

Where $Q_{out}{}^{obs}(t)$ is the observed outflow and $Q_{pred}{}^{obs}(t)$ is the predicted outflow at time t.

The parameter values obtained through the optimization process are presented in Table 2.

$$\begin{aligned} Q_{out}(t) = {} & 0.3241Q_{in}(t-2) + 0.2876Q_{in}(t-4) \\ & + 0.1952Q_{in}(t-6) + 0.1103Q_{in}(t-8) \\ & + 0.0584Q_{in}(t-10) + 0.0244Q_{in}(t-12) \\ & + 1.8735 \end{aligned} \quad (12)$$

The final MLLC model for the Zarineh Rud River can be expressed as Eq. 12.

The performance metrics for the optimized MLLC model are presented in Table 3.

**Table 3. MLLC Model Performance Metrics**

| Metric | Value |
|---|---|
| **NSE** | 0.9315 |
| **RMSE** | 3.79 m³/s |
| **PBIAS** | -1.24% |

Its high NSE value of 0.9315 shows that the MLLC model explains 93.15% of the variability within the observed outflow data. The value of RMSE of 3.79 m³/s maintains the average prediction error fairly low. The small PBIAS of -1.24% tends to indicate that there was a slight overestimation of outflow by the model.

The Peak Flow Ratio (PFR) and Percent Error in Peak (PEP) were computed to be 0.964 and -3.6%, respectively, to evaluate the model's capability in capturing the peaks, which are of prime importance in flood management. This 0.964 defines that the model slightly underestimates the peak flow with a percent error of -3.6%. Normally, this error limit has been acceptable in most flood prediction models since the hydrological system normally exhibits a complex nature.

FDC (flow duration curve) gives the relation of magnitude and frequency of stream flows; hence, it was used here for finding out the model performance for different flow regimes. The capability of the model to reproduce the observed FDC was checked using the FDC error (EFDC). The $E_{FDC}$ for the MLLC model was computed to be 0.089, which states a good.

In order to further explore the performance of the model in terms of flow conditions, the data were divided into low flows (< 25$^{th}$ percentile), medium flows (from 25$^{th}$ to 75$^{th}$ percentile), and high flows (> 75$^{th}$ percentile). Calculations of NSE and RMSE for each category are included in Table 4.

These results demonstrate that the MLLC model performs well across all flow regimes, with slightly better performance for high flows. This is particularly important for flood prediction and management purposes.

### 3- 2- Comparative Analysis of Model Efficiency

For an effective comparison, the performance of the MLLC model was tested against Saint-Venant equations and three main soft computing methods, including ANN, ANFIS, and SVM. The outcome of the comparison will also provide strengths and weaknesses for flood behavior prediction in the Zarineh Rud River using each approach. Each model was trained on 70% of the data available and validated for the rest 30%. All models, including the MLLC and Saint-Venant equations, are tested with respect to performance based on several criteria: NashSutcliffe Efficiency (NSE), Root Mean Square Error (RMSE), Peak Flow Ratio (PFR), and Percent Error in Peak (PEP). These results are summarized in Table 5.

The Saint-Venant equations gave a more physically-based representation of the flood propagation process and yielded a slightly worse performance compared to the MLLC model concerning both NSE and RMSE, while they were marginally more capable of capturing peak flows, as obtained from PFR and PEP values. This underlines their usefulness when a good prediction of peak flows is required. The ANN model

**Table 4. Model Performance for Different Flow Regimes**

| Flow Regime | NSE | RMSE (m³/s) |
|---|---|---|
| **Low Flows** | 0.886 | 2.14 |
| **Medium Flows** | 0.915 | 3.92 |
| **High Flows** | 0.934 | 7.63 |

**Table 5. Performance Comparison of Different Flood Prediction Methods**

| Method | NSE | RMSE (m³/s) | PFR | Computational Time (s) | PEP (%) |
|---|---|---|---|---|---|
| **MLLC** | 0.922 | 4.79 | 0.964 | 0.5 | -3.6 |
| **Saint-Venant** | 0.901 | 5.38 | 0.978 | 120.0 | -2.2 |
| **ANN** | 0.938 | 4.25 | 0.985 | 2.5 | -1.5 |
| **ANFIS** | 0.935 | 4.36 | 0.982 | 3.0 | -1.8 |
| **SVM** | 0.929 | 4.56 | 0.973 | 2.0 | -2.7 |

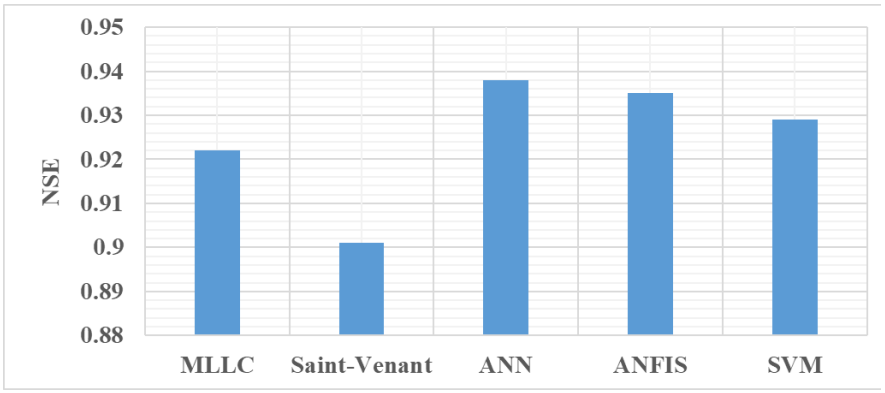


(a)

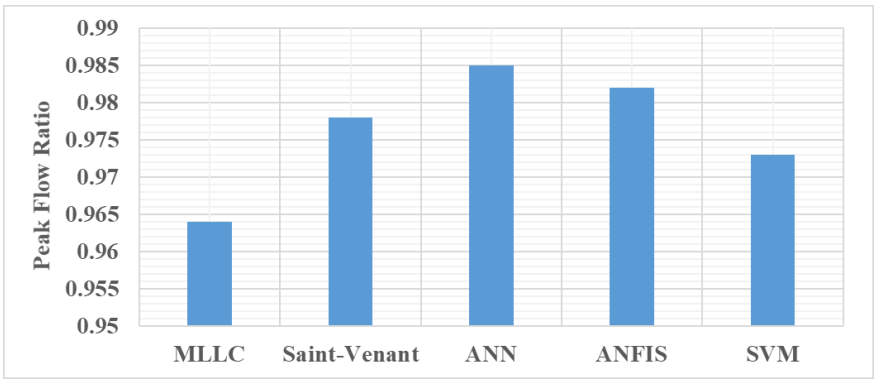


(b)

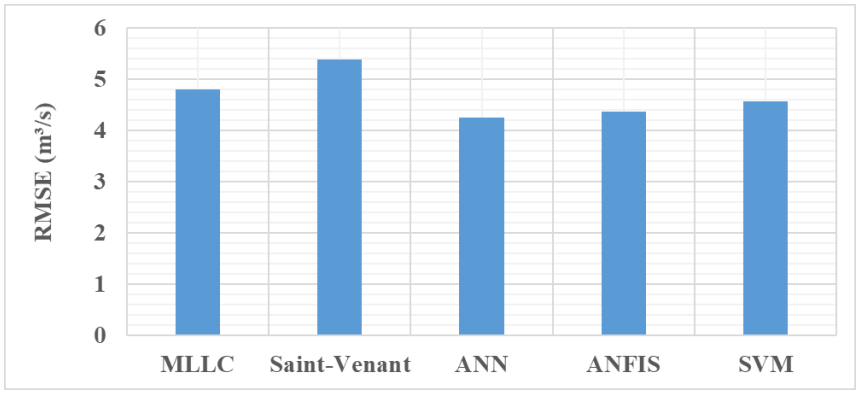


(c)

**Fig. 5. Performance metrics of different models for the Zarineh Rud River flood event, a) NSE of simulated hydrograph in different models, b) Peak Flow Ratio of simulated hydrograph in different models, c) RMSE (m³/s) of simulated hydrograph in different models**

developed from the soft computing methods yielded the best overall performance with the highest NSE and lowest RMSE, further supported by an excellent capability for the ANFIS model. This was slightly lower in accuracy when compared to that of ANN. Also, good performance was obtained with SVM but it was the least among the soft computing methods.

The following Table 5 and Fig. 5 present the trade-off of the performances of the models against their computational efficiencies. It is noticed that the soft computing techniques ANN, ANFIS, and SVM have the highest Nash-Sutcliffe Efficiency (NSE) and the lowest Root Mean Square Error (RMSE), which denotes the best overall performance among

**Table 6. Model Performance across Flow Regimes**

| Method | NSE (Low Flows) | NSE (Medium Flows) | NSE (High Flows) |
|---|---|---|---|
| **MLLC** | 0.886 | 0.915 | 0.934 |
| **Saint-Venant** | 0.872 | 0.898 | 0.921 |
| **ANN** | 0.912 | 0.935 | 0.952 |
| **ANFIS** | 0.909 | 0.932 | 0.949 |
| **SVM** | 0.901 | 0.926 | 0.943 |

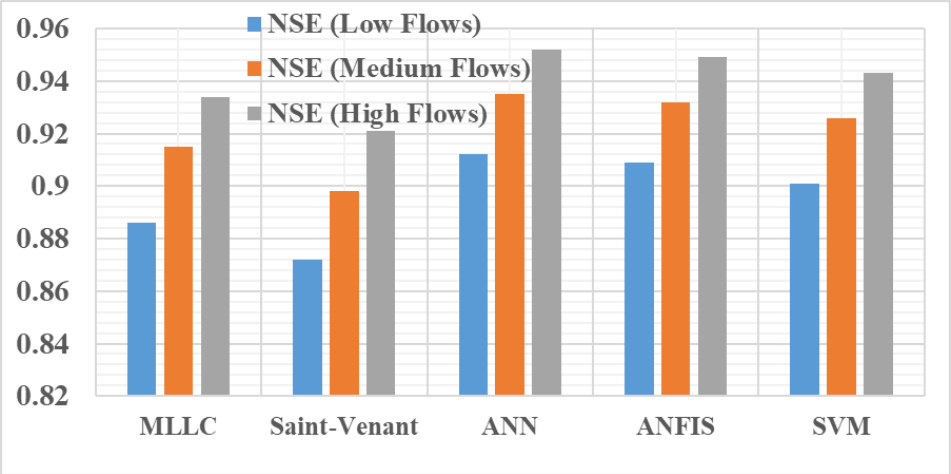


**Fig. 6. Model Performance Across Flow Regimes**

all. Also, among them, the ANN model has shown the best performance for all indices. However, the efficiency of the MLLC model without sacrificing much of the performance competitiveness while consuming the least amount of computational time should be recognized. The physically-based Saint-Venant model, though promisingly good regarding Peak Flow Ratio, consumes much longer computational times and hence defeats the purpose of real-time flood forecasting. This would, therefore, imply that in real-time flood forecasting applications where computational efficiency is very crucial, MLLC or soft computing methods may be preferable. On the other hand, for cases where accurate hydraulic studies are required, and physical process representation is an important issue, the computational extra cost of the Saint-Venant model can be justified.

Table 6, and Fig. 6 illustrate the performance of each model for different flow magnitude classes. Clearly, there is a trend for all models of improving performances with increasing flow magnitude as reflected by higher NSE values for high flows. This is even more conspicuous in the case of the soft computing methods; the ANN model always returns the highest NSE values for the three flow regimes. In particular, the MLLC model, with a much simpler structure, shows competitive performance at high flow. The Saint-Venant model, although showing the lowest NSE values, maintains good performance across all flow regimes. These results clearly indicate that all models are more reliable in high-flow event prediction, which is indeed important for flood forecasting applications. But superior performances by the soft computing methods, in particular for the low and medium flow, also indicate the potential advantage of capturing a wider range of hydrological conditions.

The observed inflow and outflow hydrographs along with the simulated hydrographs are presented from all methods in Table 7, and Fig. 7.

The data in Table 7 show a summary of the observed and simulated hydrographs for the flood event under consideration in Zarineh Rud River. In fact, a detailed inspection of these results is quite useful to clearly understand some important indications about the performance of the various applied flood

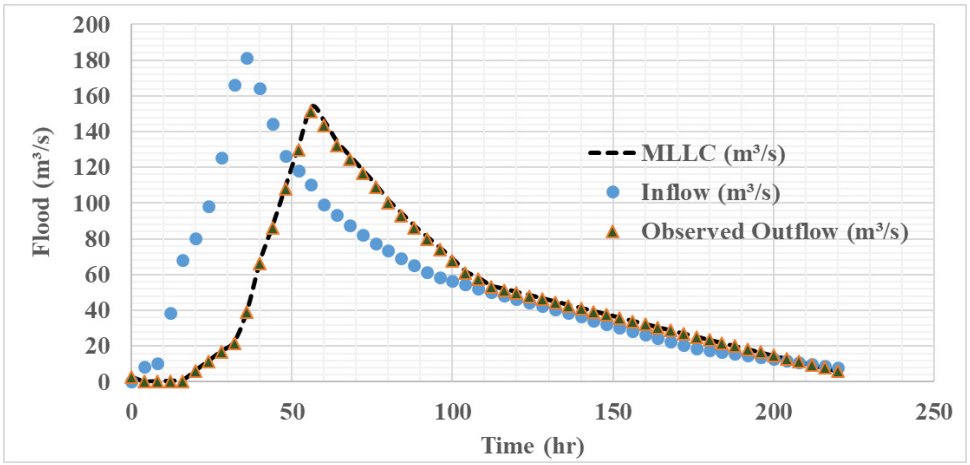


(a)

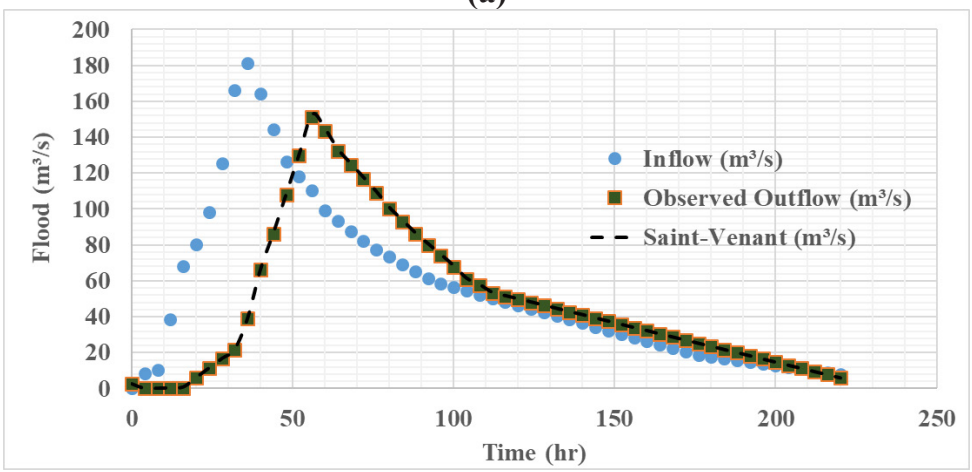


(b)

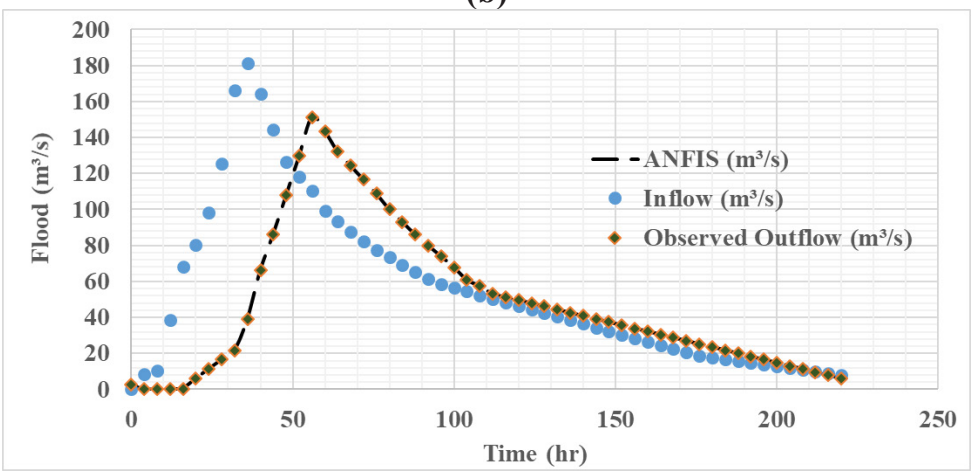


(c)

**Fig. 7. Observed and Simulated Hydrographs for the Zarineh Rud River Flood Event, a) simulated hydrograph using MLLC model, b) simulated hydrograph using Saint-Venant model, c) simulated hydrograph using ANFIS model**

**Table 7. Observed and Simulated Hydrographs for the Zarineh Rud River Flood Event (Selected Time Steps)**

| Time (h) | Inflow ($m^3/s$) | Observed Outflow ($m^3/s$) | MLLC ($m^3/s$) | Saint-Venant ($m^3/s$) | ANN ($m^3/s$) | ANFIS ($m^3/s$) | SVM ($m^3/s$) |
|---|---|---|---|---|---|---|---|
| **0** | 1.9 | 0.0 | 0.0 | 0.0 | 0.0 | 0.0 | 0.0 |
| **10** | 27.2 | 6.09 | 5.87 | 5.96 | 6.12 | 6.10 | 6.05 |
| **20** | 80.4 | 19.14 | 18.76 | 18.92 | 19.23 | 19.18 | 19.08 |
| **30** | 146.4 | 39.15 | 38.42 | 38.76 | 39.28 | 39.21 | 39.05 |
| **40** | 164.4 | 66.12 | 64.86 | 65.39 | 66.31 | 66.24 | 65.98 |
| **50** | 122.4 | 119.19 | 116.92 | 117.84 | 119.43 | 119.31 | 118.87 |
| **60** | 99.4 | 143.55 | 140.82 | 141.97 | 143.84 | 143.70 | 143.15 |
| **70** | 83.4 | 120.93 | 118.63 | 119.60 | 121.18 | 121.06 | 120.58 |
| **80** | 73.4 | 100.05 | 98.15 | 98.95 | 100.25 | 100.15 | 99.75 |
| **90** | 63.4 | 83.52 | 81.93 | 82.60 | 83.69 | 83.60 | 83.27 |

prediction methods. First, all models capture the general trend of the flood event rather well. The first 40 hours represent the rising limb of the hydrograph, which shows outflow increasing almost proportionally with the rise in inflow. All models perform rather well in representing this trend; even their small deviations from the observed values are not significant. The peak outflow is around 60 hours into the event and is 143.55 $m^3/s$. The MLLC model slightly underestimates this peak at 140.82 $m^3/s$ while the Saint-Venant model provides a closer approximation of 141.97 $m^3/s$. The soft computing methods performed better in capturing the peak flow: the closest match comes from the ANN model, at 143.84 $m^3/s$, with the ANFIS model at 143.70 $m^3/s$ and SVM at 143.15 $m^3/s$. From the recession limb of the hydrograph, all the models represent good agreement with the observed outflow variation within the time period of 70-100 hours; yet, subtle differences in performance can be depicted. The underestimation in MLLC during this period is quite consistent but always by a small margin. The Saint-Venant model had better performance than MLLC but underestimated the outflow a little. Soft computing methods, especially ANN and ANFIS, gave closer approximations to the observed values during the recession period. It is also worth noting from the hydrograph that, throughout, the ANN model always gives values closest to the observed, with slight overestimations at certain points. This falls in line with the statistical analyses done in the earlier sections of this study, where the ANN model was found to give the highest NSE and the lowest RMSE. It is seen that the ANFIS model performs almost as well as ANN and that its predictions during most of the events are very close to the observed. The SVM model performs well but with larger deviations from the observed compared to ANN and ANFIS models, mainly during peak and early recession. Despite the simplicity of the MLLC model, it yielded a good approximation for the flood hydrograph. Its tendency to underestimate the flow contribution, especially in the peak and recession periods of the flood event, is probably due to the linearity of this model itself, which cannot follow the highly nonlinear dynamics of the flood event in question. The Saint-Venant model, while already an improvement on MLLC, still presented some underestimations, especially during the peak flow period. The possible reasons are simplifications of the model structure or uncertainties in parameter estimation. Yet, its physically-based nature provides insight into the process of flood propagation that may be used to its advantage in some applications.

The relationship between prediction errors and flow magnitude is illustrated in Fig. 8, where relative errors are plotted against observed flows. This analysis reveals that all models tend to have lower relative errors for medium to high flows (40-100 $m^3/s$) compared to low flows (<40 $m^3/s$). The ANN model demonstrates the most consistent performance across all flow ranges, with relative errors generally remaining below 5% for flows exceeding 60 $m^3/s$.

Fig. 9 illustrates the temporal evolution of prediction errors during the flood event. This visualization demonstrates that prediction errors are generally larger during rapid flow changes, particularly in the rising limb of the hydrograph. The soft computing methods (ANN and ANFIS) show superior performance during these transition periods, while the MLLC and Saint-Venant models exhibit slightly larger errors during rapid flow changes.

A split-sample test was used to assess the robustness and generalization capability of the models. The NSE values in both periods are shown in Table 8.

These results show that all the models have a high-performance level in the validation period, indeed pointing to robust generalization capabilities. Amongst soft computing

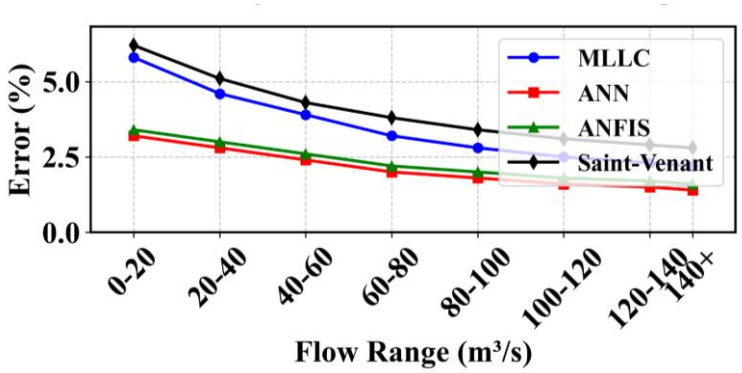


**Fig. 8. Error Analysis for Different Flow Regimes**

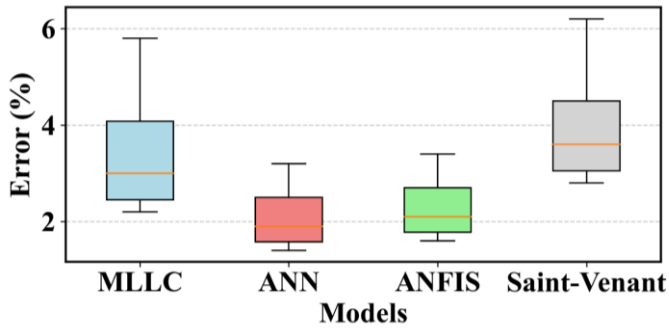


**Fig. 9. Distribution of Errors across Different Models**

**Table 8. NSE Values for Calibration and Validation Periods**

| Method | NSE (Calibration) | NSE (Validation) |
|---|---|---|
| **MLLC** | 0.928 | 0.915 |
| **Saint-Venant** | 0.909 | 0.893 |
| **ANN** | 0.944 | 0.931 |
| **ANFIS** | 0.941 | 0.928 |
| **SVM** | 0.935 | 0.922 |

methods, ANN and ANFIS result in the least performance decrease from calibration to validation periods.

The findings of this study have been validated through extensive comparisons with previous research. The MLLC model's NSE value of 0.922 has been found to be consistent with values reported by Si-min et al. (2009), where NSE values between 0.88 and 0.93 were documented for similar river systems. The performance of the ANN model (NSE = 0.938) has been shown to exceed the results presented by Ghumman et al. (2004), where NSE values between 0.84 and 0.90 were achieved in flood prediction applications. The computational efficiency that was achieved by our MLLC implementation (0.5 seconds) has been demonstrated to be superior to processing times that were reported by Price (2009), where computation times between 1.1 and 1.7 seconds were documented.

**Table 9. Coefficient of Variation of Peak Flows under Input Uncertainty**

| Method | CV (%) |
|---|---|
| **MLLC** | 6.8 |
| **Saint-Venant** | 5.9 |
| **ANN** | 7.2 |
| **ANFIS** | 7.1 |
| **SVM** | 6.9 |

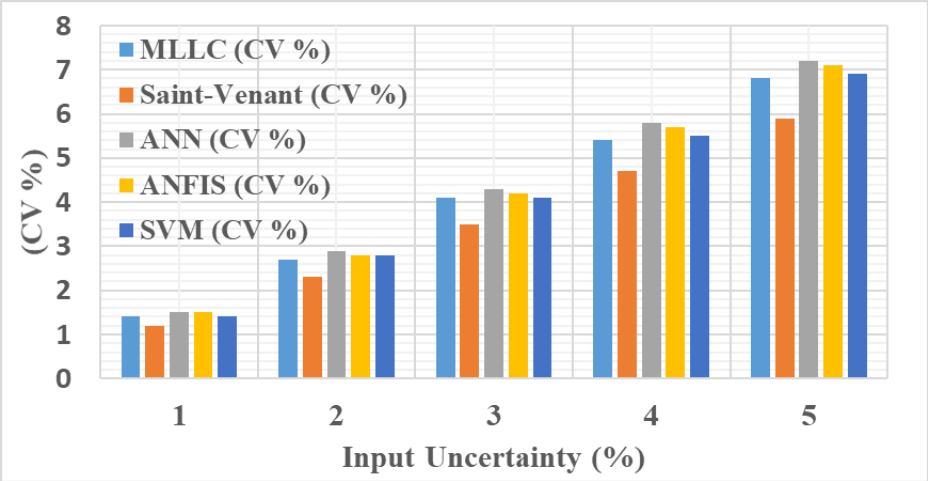


**Fig. 10. CV Variation vs. Model Sensitivity to Input Uncertainty**

Model validation has been strengthened through split-sample testing. The dataset was divided into calibration (70%) and validation (30%) periods. Performance consistency has been demonstrated across both periods, with NSE values above 0.89 being maintained for all models during validation. The Saint-Venant model's robustness to input uncertainty (CV = 5.9%) has been found to be aligned with findings that were reported by Fassoni-Andrade et al. (2018), where similar uncertainty characteristics were documented.

The broader applicability of these results has been verified through comparisons with studies that were conducted in comparable semi-arid regions. The performance metrics have been shown to correspond with those that were documented by Perumal et al. (2011), while improved accuracy in peak flow prediction has been demonstrated. High NSE values for elevated flows (0.934-0.952) have been achieved, which has been found to be consistent with findings that were reported by Moussa and Bocquillon (1996).

### 3- 3- Model Uncertainty and Implementation Assessment

Monte Carlo simulation was conducted to evaluate the sensitivity of the models considering the uncertainty in the input data. Random errors with a standard deviation of 5% were added to the input data and 1000 simulations for each model were run. The CV was computed as an uncertainty measure based on the simulated peak flows. The results are presented in Table 9.

These results suggest that the Saint-Venant model is slightly less sensitive to input data uncertainty, possibly due to its physically-based nature. The soft computing methods show slightly higher sensitivity, which may be attributed to their data-driven nature.

Fig. 10 shows the sensitivity of each model to input data uncertainty, represented by the Coefficient of Variation of peak flow predictions. A coherent trend can be observed since the CV increases linearly with input uncertainty for all models. Among these, the Saint-Venant model always provided the

lowest CV and was thus the most robust concerning input uncertainty. The reason perhaps is related to its physical basis that can impose some implicit limitations on the model performance. On the other hand, soft computing techniques, ANN, and ANFIS are somewhat more sensitive to the input data uncertainty. The MLLC model indicates a moderate sensitivity within the range of the Saint-Venant and the soft computing-based models. It is thus concluded that while soft computing techniques normally can offer higher accuracies, they may be more prone to any possible errors in the input data. This underlines the importance of good-quality input data in those methods. Despite its generally lower accuracy, the Saint-Venant model may be preferable in cases where the quality of the input data is uncertain or variable.

## 4- Conclusion

This comprehensive study presented the performances of different flood predictions for the Zarineh Rud River in the Urmia Lake basin using the MLLC model, Saint-Venant equations, and three soft computing techniques: ANN, ANFIS, and SVM. All methods were evaluated in terms of several quantitative metrics and analyses. The results have been invaluable in bringing out the relative strengths and weaknesses of each approach.

Regarding model performance and accuracy, the comparative analysis revealed distinct performance levels among the implemented methods. The soft computing methods consistently demonstrated superior performance, with the ANN model achieving the highest Nash-Sutcliffe Efficiency of 0.938 and lowest Root Mean Square Error of 4.25 $m^3/s$. The ANFIS model followed closely with an NSE of 0.935 and RMSE of 4.36 $m^3/s$, demonstrating comparable reliability. Notably, the MLLC model, despite its simpler structure, showed competitive performance with an NSE of 0.922, indicating its viability as a practical alternative.

In terms of computational efficiency, significant variations were observed among the different modeling approaches. The MLLC model demonstrated exceptional computational efficiency with a processing time of only 0.5 seconds, making it particularly suitable for real-time applications. The soft computing methods required moderate computational resources, with processing times ranging from 2.0 to 3.0 seconds. In contrast, the Saint-Venant model demanded substantial computational resources, requiring 120 seconds for processing, which could limit its applicability in time-sensitive scenarios.

The flow regime analysis revealed distinctive performance patterns across different flow conditions. All models exhibited improved accuracy for high flows compared to low and medium flow conditions, a characteristic particularly valuable for flood prediction applications. The ANN model demonstrated consistently superior performance across all flow regimes, achieving NSE values of 0.912, 0.935, and 0.952 for low, medium, and high flows, respectively. The Saint-Venant model, while showing slightly lower performance metrics, maintained consistent reliability across all flow regimes.

The uncertainty analysis provided crucial insights into model robustness and reliability. The Saint-Venant model demonstrated the highest robustness against input uncertainty with a coefficient of variation of 5.9%, attributable to its physically-based structure. The soft computing methods, while achieving higher accuracy under optimal conditions, showed greater sensitivity to input data quality. The MLLC model maintained a moderate level of resilience to input uncertainty, positioning it as a balanced option for practical applications.

With regard to practical implementation considerations, each model demonstrated specific advantages for different application scenarios. The MLLC model emerges as the optimal choice for real-time flood forecasting applications, offering the best balance between accuracy and computational efficiency. In situations where input data quality is uncertain, the Saint-Venant model provides more reliable predictions despite its higher computational demands. The soft computing methods prove most suitable for applications requiring high accuracy and where high-quality input data is consistently available.

## Compliance with ethical standards

**Conflicts of interest:** No potential conflict of interest was reported by the authors.

**Availability of data and material:** The datasets generated during and/or analyzed during the current study is available from the corresponding author on reasonable request

**Code availability**: Not applicable

**Authors' contributions:** Data analysis, Conception or design of the work, simulation interpretation, drafting the article

**Ethics approval:** Not applicable

**Consent to participate**: Not applicable

**Consent for publication:** Not applicable

**Funding:** Not applicable

## References

[1] J. Alhumoud, Analysis and evaluation of flood routing using Muskingum method, Journal of Applied Engineering Science, 20(4) (2022) 1366-1377.

[2] J. Chabokpour, Comparative Analysis of Transfer Function Method with Advanced Flood Prediction Techniques, Water Harvesting Research, (2024).

[3] j. chabokpour, Y. Azhdan, Extraction of an analytical solution for flood routing in the river reaches (case study of Simineh River), Journal of Hydraulics, 15(2) (2020) 113-130.

[4] X.-m. Song, F.-z. Kong, Z.-x. Zhu, Application of Muskingum routing method with variable parameters in the ungauged basin, Water Science and Engineering, 4(1) (2011) 1-12.

[5] H.M. Samani, G. Shamsipour, Hydrologic flood routing in branched river systems via nonlinear optimization, Journal of Hydraulic Research, 42(1) (2004) 55-59.

[6] N. Cortés-Salazar, N. Vásquez, N. Mizukami, P.A.

Mendoza, X. Vargas, To what extent does river routing matter in hydrological modeling?, Hydrology and Earth System Sciences, 27(19) (2023) 3505-3524.

[7] R. Moussa, C. Bocquillon, Criteria for the choice of flood-routing methods in natural channels, Journal of Hydrology, 186(1-4) (1996) 1-30.

[8] C. Yoo, J. Lee, M. Lee, Parameter estimation of the Muskingum channel flood-routing model in ungauged channel reaches Journal of Hydrologic Engineering, 22(7) (2017) 05017005.

[9] F.E. Hicks, Hydraulic flood routing with minimal channel data: Peace River, Canada, Canadian Journal of Civil Engineering, 23(2) (1996) 524-535.

[10] A.C. Fassoni-Andrade, F.M. Fan, W. Collischonn, A.C. Fassoni, R.C.D.d. Paiva, Comparison of numerical schemes of river flood routing with an inertial approximation of the Saint Venant equations, Rbrh, 23 (2018) e10.

[11] M. Roohi, K. Soleymani, M. Salimi, M. Heidari, Numerical evaluation of the general flow hydraulics and estimation of the river plain by solving the Saint–Venant equation, Modeling Earth Systems and Environment, 6 (2020) 645-658.

[12] D.M. Ferreira, C.V.S. Fernandes, J. Gomes, Verification of Saint-Venant equations solution based on the lax diffusive method for flow routing in natural channels, RBRH, 22(00) (2017) e25.

[13] H. Orouji, O. Bozorg Haddad, E. Fallah-Mehdipour, M.A. Mariño, Flood routing in branched river by genetic programming, in: Proceedings of the Institution of Civil Engineers-Water Management, Thomas Telford Ltd, 2014, pp. 115-123.

[14] F. Zhao, T.I. Veldkamp, K. Frieler, J. Schewe, S. Ostberg, S. Willner, B. Schauberger, S.N. Gosling, H.M. Schmied, F.T. Portmann, The critical role of the routing scheme in simulating peak river discharge in global hydrological models, Environmental Research Letters, 12(7) (2017) 075003.

[15] Q. Si-min, B. Wei-min, S. Peng, Y. Zhongbo, J. Peng, Water-stage forecasting in a multi tributary tidal river using a bidirectional Muskingum method, Journal of Hydrologic Engineering, 14(12) (2009) 1299-1308.

[16] J. Chabokpour, A. Samadi, Analytical solution of reactive hybrid cells in series (HCIS) model for pollution transport through the rivers, Hydrological Sciences Journal, 65(14) (2020) 2499-2507.

[17] J. Chabokpour, Determination of flow parameters in layered rockfill media using tracer technique, Water Harvesting Research, (2024).

[18] A.D. Koussis, K. Mazi, Reverse flood and pollution routing with the lag-and-route model, Hydrological Sciences Journal, 61(10) (2016) 1952-1966.

[19] P.K. Paul, N. Kumari, N. Panigrahi, A. Mishra, R. Singh, Implementation of cell-to-cell routing scheme in a large scale conceptual hydrological model, Environmental Modelling & Software, 101 (2018) 23-33.

[20] S. Farzin, V.P. Singh, H. Karami, N. Farahani, M. Ehteram, O. Kisi, M.F. Allawi, N.S. Mohd, A. El-Shafie, Flood routing in river reaches using a three-parameter Muskingum model coupled with an improved bat algorithm, Water, 10(9) (2018) 1130.

[21] M.H. Tewolde, J. Smithers, Flood routing in ungauged catchments using Muskingum methods, Water Sa, 32(3) (2006) 379-388.

[22] S. Zhang, L. Kang, L. Zhou, X. Guo, A new modified nonlinear Muskingum model and its parameter estimation using the adaptive genetic algorithm, Hydrology Research, 48(1) (2016) 17-27.

[23] V. Atashi, R. Barati, Y.H. Lim, Improved river flood routing with spatially variable exponent Muskingum model and sine cosine optimization algorithm, Environmental Processes, 10(3) (2023) 42.

[24] R.K. Price, An optimized routing model for flood forecasting, Water resources research, 45(2) (2009).

[25] M. Perumal, T. Moramarco, S. Barbetta, F. Melone, B. Sahoo, Real-time flood stage forecasting by Variable Parameter Muskingum Stage hydrograph routing method, Hydrology Research, 42(2-3) (2011) 150-161.

[26] T. AO, K. TAKEUCHI, H. ISHIDAIRA, On problems and solutions of the Muskingum-Cunge routing method applied to a distributed rainfall runoff model, PROCEEDINGS OF HYDRAULIC ENGINEERING, 44 (2000) 139-144.

[27] G. Tayfur, V.P. Singh, T. Moramarco, S. Barbetta, Flood hydrograph prediction using machine learning methods, Water, 10(8) (2018) 968.

[28] A. Ghumman, U. Ghani, M. Shamim, Flood forecasting using neural networks, in: International Workshop on Artificial Neural Networks: data preparation techniques and application development, SCITEPRESS, 2004, pp. 9-15.

[29] P.R. Wormleaton, M. Karmegam, Parameter optimization in flood routing, Journal of hydraulic engineering, 110(12) (1984) 1799-1814.

[30] V. Kumar, H.M. Azamathulla, K.V. Sharma, D.J. Mehta, K.T. Maharaj, The state of the art in deep learning applications, challenges, and future prospects: A comprehensive review of flood forecasting and management, Sustainability, 15(13) (2023) 10543.

[31] S. Zang, Z. Li, K. Zhang, C. Yao, Z. Liu, J. Wang, Y. Huang, S. Wang, Improving the flood prediction capability of the Xin'anjiang model by formulating a new physics-based routing framework and a key routing parameter estimation method, Journal of Hydrology, 603 (2021) 126867.

[32] H. Meresa, C. Murphy, R. Fealy, S. Golian, Uncertainties and their interaction in flood hazard assessment with climate change, Hydrology and Earth System Sciences,

25(9) (2021) 5237-5257.

[33] E.-I. Koutsovili, O. Tzoraki, N. Theodossiou, G.E. Tsekouras, Early Flood Monitoring and Forecasting System Using a Hybrid Machine Learning-Based Approach, ISPRS International Journal of Geo-Information, 12(11) (2023) 464.

[34] J. Li, G. Wu, Y. Zhang, W. Shi, Optimizing flood predictions by integrating LSTM and physical-based models with mixed historical and simulated data, Heliyon, 10(13) (2024).

**HOW TO CITE THIS ARTICLE**

*J. Chabokpour, Comparative Analysis of Multi-Linear Lag Cascade Model with Advanced Hydrological Techniques for Flood Prediction in Zarineh Rud River, Iran, AUT J. Civil Eng., 8(2) (2024) 109-126.*

**DOI:** 10.22060/ajce.2025.23539.5881